



HAL
open science

AGEING AND TEMPERING OF FERROUS MARTENSITES

Li Chang, G. Smith, G. Olson

► **To cite this version:**

Li Chang, G. Smith, G. Olson. AGEING AND TEMPERING OF FERROUS MARTENSITES. Journal de Physique Colloques, 1986, 47 (C2), pp.C2-265-C2-275. 10.1051/jphyscol:1986240 . jpa-00225674

HAL Id: jpa-00225674

<https://hal.science/jpa-00225674>

Submitted on 4 Feb 2008

HAL is a multi-disciplinary open access archive for the deposit and dissemination of scientific research documents, whether they are published or not. The documents may come from teaching and research institutions in France or abroad, or from public or private research centers.

L'archive ouverte pluridisciplinaire **HAL**, est destinée au dépôt et à la diffusion de documents scientifiques de niveau recherche, publiés ou non, émanant des établissements d'enseignement et de recherche français ou étrangers, des laboratoires publics ou privés.

AGEING AND TEMPERING OF FERROUS MARTENSITES

LI CHANG, G.D.W. SMITH and G.B. OLSON*

Department of Metallurgy and Science of Materials, University of Oxford, Parks Road, GB-Oxford OX1 3PH, Great Britain

**Department of Materials Science and Engineering, M.I.T., Cambridge, M. 02139, U.S.A.*

Abstract The low temperature ageing of a Fe-15wt%Ni-1wt%C martensite (M_s temperature -35 C) has been investigated using field-ion microscopy and atom probe microanalytical techniques. It is demonstrated that both the amplitude and the wavelength of the carbon composition fluctuations observed during room-temperature ageing increase with time, indicating that the alloy decomposes by a spinodal process. The carbon-rich regions approach a limiting composition of Fe₃C during this reaction.

The tempering behaviour of a high-cobalt-nickel secondary hardening steel, AF 1410, was also studied. The composition of the fine M_2C carbides formed during the standard tempering treatment at 510 C was determined, and coarser particles of M_2C and MC formed during overaging at 593 C were also analyzed. Some evidence of atomic ordering was observed in the Fe-Ni-Co-rich matrix; such an effect would help to explain the high resistance to dislocation recovery which is observed in this class of steels.

1 - INTRODUCTION

It has recently been demonstrated that field ion microscopy (FIM), in conjunction with atom probe microanalysis (AP), is an extremely powerful tool for the investigation of ageing and tempering processes in ferrous martensites (1-6). The dense, complex microstructures produced in martensitic steels are ideally suited for study in the FIM, and the ability of the AP to analyse quantitatively for carbon gives it a unique capability for probing the chemical nature of the decomposition processes which occur during heat treatment. At the 31st International Field Emission Symposium, we reported the first results of a study of the room temperature ageing of Fe-Ni-C martensites (6), which indicated that a spinodal decomposition reaction may be occurring. In the current paper, we present additional results, obtained over a wider range of ageing conditions, which confirm this interpretation and provide a basis for a more quantitative interpretation of the phenomenon. We also report a preliminary study of the tempering reactions occurring in a complex secondary hardening steel, AF 1410, which is of interest because of its outstanding combination of strength and toughness.

2 - EXPERIMENTAL

All work was carried out using the Oxford FIM 100 atom probe (7). Experimental procedures were as described previously (6). All analyses were carried out using a pulse fraction (pulse voltage/d.c. standing voltage) of 15%. Specimen blanks were usually heat treated and aged or tempered prior to final polishing to form FIM tips. However, in order to study the distribution of carbon atoms in virgin martensite, some specimens of the Fe-15wt%Ni-1wt%C alloy (M_s temperature -35 C) were prepared in the metastable austenitic state, and were subsequently quenched in situ in the atom probe to form martensite, which was then analysed immediately.

3 - STUDIES OF FE-15wt%Ni-1wt%C STEEL

The use of martensites of low M_s temperature is essential for the investigation of low-temperature ageing phenomena, in order to avoid the problem of auto-tempering during quenching. High-nickel alloys have been widely employed for this purpose, and here we report some extensions to previous atom probe studies of these materials (5,6).

(a) Virgin martensite Earlier work (5,6) has shown the occurrence of carbon cluster ions of the type C_2^+ , C_3^+ , C_3^{++} , etc., in the mass spectra of freshly formed martensites. It is of importance to establish whether such clusters are genuine features of virgin martensites, or if they are artefacts of the AP analysis method. In order to investigate this further, freshly-quenched specimens of the Fe-Ni-C martensite were analysed at each of 100K and 50 K. At least 10,000 ions were collected from each specimen under each set of experimental conditions. The results of the individual experiments are shown in Table I, and the percentage distributions of the various carbon ion species are summarised in Table II. The 'corrected' values of overall carbon concentration listed in Table I refer to values derived by applying a statistical analysis to take account of the pile-up of ions of the same mass-to-charge ratio at the detector in the high-resolution atom probe (7). This effect is greater at lower temperatures, where the field evaporation rate is less regular. Carbon cluster ions are evident both at 50 K and 100 K, being significantly more abundant at the higher temperature. This suggests that very localised atom movements on the specimen surface may be responsible for their formation, although the results are not conclusive in this respect. Analyses recorded at 50 K appear to show a marginally higher total carbon content, even after statistical correction of the data. However, there is some ambiguity in peak assignments, since (e.g.) C^+ and C_2^{++} species occur at the same mass-to-charge ratio. For convenience in handling the data, it is generally assumed that each peak consists only of the species of lowest mass number. This leads to a slight underestimation of the total carbon, and the discrepancy will increase as the proportion of cluster ions in the analysis increases. The additional error is clearly small.

(b) Room temperature ageing Neon FIM images of the virgin martensite and of material aged for 10 days at room temperature are shown in Figs 1 and 2 respectively. The emergence of periodic darkly-imaging areas on ageing can be clearly seen. It has previously been demonstrated that these correspond to carbon-rich regions (5,6). The evolution of the carbon composition fluctuations in these regions has now been studied in detail for ageing times of up to 68 days. The maximum amplitudes of the concentration variations have been obtained from analysis of composition-depth profiles, and the wavelengths of the fluctuations as well as the volume fractions and particle sizes of the carbon-rich areas have been obtained from autocorrelation analysis of the data (8). The results are summarised in Figs. 3 and 4. The very earliest stages of the decomposition reaction are difficult to follow, because of statistical limitations, and because of the existence of carbon cluster ions in the analyses (see above). However, it is clear that two broad regimes exist. In the first stage, at ageing times below about 200 hours, the amplitude of the composition fluctuations increases progressively, while the wavelength changes very little. In the second stage, at longer times, the amplitude of the fluctuations saturates at a composition corresponding closely to Fe_3C , and the wavelength increases progressively with time (with a time exponent of approximately $1/3$). The results are in excellent agreement with those from a parallel high-resolution electron microscopy study by Taylor (9), and demonstrate unambiguously that a spinodal decomposition reaction is occurring. This is probably the first time that such a reaction process has been positively identified in an interstitial alloy system.

(c) Ageing at higher temperatures A number of ageing treatments have been carried out at temperatures above room temperature, extending the earlier work of Miller et al (5). The results of these studies are summarised in Table III. As the temperature is raised, an increasing proportion of the high-carbon regions show maximum carbon concentrations in excess of 15 at% C, indicating that a further stage of

decomposition is occurring. It is clear from the electron microscopy work of Taylor (9) that this stage corresponds to nucleation and growth of the epsilon carbide phase. The atom probe results confirm that there is a range of ageing times and temperatures over which the carbon-rich Fe₃C regions coexist (unstably) with the epsilon phase. Although the competition between these decomposition reactions complicates the determination of the metastable miscibility gap underlying the spinodal reaction, the results thusfar indicate that the Fe₃C composition of the high carbon phase boundary is temperature insensitive over the range examined. Further controlled ageing studies over a range of temperatures and alloy carbon contents are underway to clarify the metastable phase relations in this important system.

4. AF 1410 STEEL

The secondary hardening steel AF 1410 has the composition Fe-14wt%Co-10wt%Ni-2wt%Cr-1wt%Mo-0.15wt%C (equivalent to Fe-13.5at%Co-9.7at%Ni-2.2at%Cr-0.6at%Mo-0.7at%C). It belongs to a relatively new class of high-cobalt-nickel alloys which exhibit outstanding combinations of strength and toughness in the tempered state. One effect of cobalt is to retard the rate of recovery of the dislocation substructure of the as-quenched martensite, leading to the formation of an exceptionally fine dispersion of secondary carbides during the tempering process (10). The mechanism by which cobalt retards recovery is unknown, although one suggestion is that a form of short-range order may be present in the ferrite matrix, which would be expected to inhibit dislocation climb. It is of interest to investigate this point using the FIM/AP technique, and also to study the evolution of the phase chemistry of the complex secondary carbides formed during tempering, which might provide a further clue to the stability of the microstructure. We report here a preliminary study of AF 1410, after the standard tempering treatment (5h at 510 C), and after an additional over-ageing treatment (24h at 593 C).

(a) FIM images Neon FIM images of the steel in the standard and overaged condition are shown in Figs 5-7. The main features of the microstructure are: 1. carbide particles which have the brightest contrast due to the presence of Mo atoms, 2. boundaries which have dark line contrast, and 3. contrast features from the ferrite matrix.

Carbide particles can be seen most clearly in images taken at voltages below best image voltage and at temperatures above 80 K, Fig. 5. At lower temperatures and at higher image voltages, the carbide contrast is much reduced, Fig. 6. The carbides formed after the standard heat treatment are needle-like. Those needles lying parallel to the specimen surface exhibit an array of brighter spots on the image, Fig. 5a, while the rest only appear as one or two bright spots, Fig 5b. The average particle size in this condition is about 3nm long and 0.5-0.8 nm in diameter. The estimated density of such particles is of the order of 10^{18} cm⁻³. The interparticle spacing is about 5 nm. Coarse carbides are easily observed in overaged specimens, and are around 10 nm in diameter, Fig. 7.

The boundaries are lath or possibly twin boundaries from the original martensitic substructure. Some boundaries of this kind can be seen in the micrograph of Fig. 5b, running diagonally across the image, and about 5 nm apart.

FIM images taken at 50 K show that some areas in the matrix have double rings at the low index poles, for example the central low-index plane of Fig. 6a. Also, in some cases a very regular, localised two-dimensional array of image spots is seen, for example at the extreme left of the micrograph of Fig. 6b. This suggests that some ordering of the matrix may have taken place during tempering. Because of the limited extent of such regions, it is possible that this may be a form of short-range order in which localised regions attain a very high degree of regularity. An effect of this kind has already been postulated to occur in the case of binary Fe-Co alloys, on the basis of neutron diffraction evidence (11), and a similar effect has also been suggested in maraging steels (12).

(b) Atom probe analysis The matrix. Typical matrix compositions are given in Table IV. Co and Ni account for about 25% of the matrix. The presence of Cr in the matrix indicates that not all of this element has been incorporated into the carbide phase. Detailed analysis showed that there was some Cr segregation at martensite boundaries. The Cr enriched boundaries may contain more than 3% Cr over a 2 nm wide area, and the local concentration could be much higher if most Cr atoms were localised at the plane of the boundary. No significant variations of solute content in the matrix have been detected between standard and overaged conditions. Although Cr should be soluble in Fe-Co-Ni alloys, Cr segregation might be promoted by ordering, which could involve the rejection of Cr from the ordered regions. Unfortunately, no well-ordered regions have so far been analysed, so their composition remains unknown. Mo, a strong carbide forming element, has apparently gone virtually completely into the carbide phase, since no Mo has been detected in the matrix in either heat treatment condition.

Carbides Table V gives the measured carbide compositions. In the standard heat-treatment condition, since the carbides are smaller than the size of the probe hole, it is inevitable that ions from the matrix are collected during probing of the carbide. If the matrix contribution is subtracted, assuming no Ni and Co in the carbide, and taking the matrix composition to be as given in Table IV, the result is very close to the M_2C composition. The ratio of Cr:Mo:Fe is about 1.3:1:0.8. A similar ratio in M_2C carbide has also been obtained by Stiller et al in an atom probe study of a high-speed tool steel (13).

Two kinds of carbides have been detected in overaged specimens. One is a coarsened form of the M_2C carbide which is Cr-rich with a Cr:Mo ratio of 1.0-1.8 and a much reduced Fe content compared to the M_2C carbides in the standard heat treatment condition. The other appears to be a carbon-deficient MC, which is a Mo-rich carbide with a Cr:Mo ratio of 0.4-0.6. Typical mass spectra from each type of carbide are shown in Fig. 8. The observation of decreasing Fe content of alloy carbides with increased ageing, and the different Cr:Mo ratios of M_2C and MC carbides are in excellent agreement with the results of Stiller et al (13), for a somewhat similar secondary hardening steel.

From the Cr:Mo ratios in the carbides and the fact that apparently all the Mo is in the carbides, only half of the Cr of the bulk composition stays in alloy carbides, and the rest of the Cr, (1%), should then be in the matrix. This agrees well with the matrix analyses, Table IV. Pilling and Ridley (14) have shown that the Mo:Cr ratio in M_2C decreases with carbon concentration in a 2.25wt%Cr-1wt%Mo low carbon steel, and increases with tempering time. Hence a certain amount of Cr, dependent on the ratio of Mo:C in the bulk, can act as a carbide-former, together with Mo in M_2C carbide. This solubility of Cr in M_2C , together with a higher diffusivity of Cr relative to Mo can explain why a Cr addition shifts the secondary hardening peak in 10Ni-8Co-1Mo-0.12C steels to lower temperature, as Speich et al have demonstrated (10). Excess Cr in the matrix could also have an important role, for example via solid solution strengthening, or by segregation, which might impede matrix recovery processes. Further studies are needed in order to determine the relative importance of these effects, and to assist in the design of improved steels of this type, which may well prove to be of major importance in a number of critical engineering applications.

Acknowledgements

This work was supported by the Science and Engineering Research Council (U.K.); research at M.I.T. on martensite ageing phenomena and secondary hardening mechanisms is supported by the Office of Naval Research and the National Science Foundation (U.S.A.), respectively. Li Chang wishes to thank the Government of the Republic of China (Taiwan) for a postgraduate scholarship.

References

1. Miller M.K., Beaven P.A., Lewis R.J. and Smith G.D.W., *Surface Sci.*, 70, (1978), 470.
2. Miller M.K., Beaven P.A. and Smith G.D.W., *Met. Trans.A*, 12A, (1981), 1197.
3. Barnard S.J., Smith G.D.W., Sarikaya M. and Thomas G., *Scripta Met.* 15, (1981), 387.
4. Thomas G., Sarikaya M., Smith G.D.W. and Barnard S.J., *Proc. Conf. on Advances in the Physical Metallurgy and Applications of Steels*, publ. The Metals Society (London) 1983, p. 1421.
5. Miller M.K., Beaven P.A., Brenner S.S. and Smith G.D.W., *Met. Trans. A*, 14A, (1983), 1021.
6. Chang L., Cerezo A., Smith G.D.W., Miller M.K., Burke M.G., Brenner S.S., Taylor K.A., Abe T. and Olson G.B., *J. de Physique, Colloq. C9*, suppl. to vol 45, (1984), 409.
7. Cerezo A., Smith G.D.W. and Waugh A.R., *J. de Physique, Colloq. C9*, suppl to vol 45, (1984), 329.
8. Piller J. and Wendt H., *Proc. 29th Intl. Field Emission Symposium, Gothenburg 1982*, eds. Andren H-O. and Norden H., publ. Almqvist and Wiksell, Stockholm, Sweden 1982, p. 265.
9. Taylor K.A., Sc.D. Thesis, M.I.T. June 1985 (unpublished).
10. Speich G.R., Dabkowski D.S. and Porter L.F., *Met. Trans.*, 4, (1973), 30.
11. Pierron-Bohnes V., Cadeville M.C., and Parette G., *J. Phys. F: Met. Phys.*, 15, (1985), 1441.
12. Spooner S., Rack H.J., and Kalish D., *Met. Trans.* 2, (1971), 2306.
13. Stiller K., Svensson L-E., Howell P.R., Rong W., Andren H-O. and Dunlop G.L., *Acta Met.*, 32, (1984), 1457.
14. Pilling J., and Ridley N., *Met. Trans. A*, 13A, (1982) 557.

Table I: Composition of As-quenched Fe-Ni-C Martensite

Specimen	Total Carbon Concentration (atom pct)		Atom pct of Carbon Ion Species having various mass-Co-charge ratios (in Total Carbon Atoms)				
	<u>Uncorrected</u>	<u>Corrected</u>	C ₆	C ₁₂	C ₂₄	C ₁₈ +C ₃₆	C ₆ +C ₁₂
	%C	%C					
1.H*	4.44 ±0.16	3.76	27.3 ±1.6	18.5 ±1.4	22.7 ±1.5	31.5 ±1.7	45.8 ±1.8
1.N*	3.92 ±0.12	3.41	31.5 ±1.4	16.3 ±1.1	19.7 ±1.2	32.5 ±1.4	47.8 ±1.5
2.N	3.75 ±0.17	3.35	23.1 ±1.9	13.9 ±1.6	22.0 ±1.9	41.0 ±2.2	37.0 ±2.2
2.H	4.29 ±0.18	3.50	36.7 ±2.1	20.9 ±1.7	17.8 ±1.6	24.6 ±1.8	57.6 ±2.1
3.H	4.40 ±0.19	3.60	35.3 ±2.1	19.0 ±1.7	22.7 ±1.8	23.0 ±1.8	54.3 ±2.2
4.N	3.92 ±0.16	--	26.0 ±1.9	18.5 ±1.7	20.9 ±1.7	34.6 ±2.0	44.5 ±2.1

* H = cold helium gas cooling, 50°K; N = liquid nitrogen cooling, 100°K. The data from specimen 1 were collected first at 50°K and then at 100°K, whereas specimen 2 was examined in reverse sequence.

Table II: Comparison of Carbon Ion Distributions at 50°K and 100°K

Temperature	Total No. of Carbon Atoms	C ₆	C ₁₂	C ₁₈ + C ₃₆	C ₂₄
100°K	1098	346	179	357	216
	490	113	68	201	108
	546	142	101	189	114
Total	2134	601	348	747	438
Percentage		28.2	16.3	35.0	20.5
50°K	733	200	136	231	166
	550	202	115	135	98
	521	184	99	120	118
Total	1804	586	350	486	382
Percentage		32.5	19.4	26.9	21.2

Table III: Selected Area Atom Probe Analysis of Fe-Ni-C Martensite aged at different temperatures (At.Pct Carbon)

Ageing Treatment	Matrix	Dark Areas Min-Max	Total Cases,	Cases <15%, >15%	
95°C/1 h	0.17-0.62	10.1-15.6	11	10	1
100°C/24 h	0.12-0.46	11.4-23.4	9	6	3
130°C/1 h	0.12-0.17	9.51-25.3	48	19	29
150°C/1 h	0.20-0.38	12.9-28.6	10	2	8

Table IV: AF 1410 Matrix Composition, at%

	Cr	Ni	Co	Fe	Si	C	Total ions
standard	1.01 ±0.33	10.39 ±1.02	14.75 ±1.19	73.74 ±1.47	0.11 ±0.11	-	893
overaged	0.98 ±0.31	8.69 ±0.88	15.82 ±1.14	74.49 ±1.49	0.11 ±0.01	0.01 ±0.01	1024

Table V: AF 1410 Carbide compositions, at%

		C	Cr	Mo	Fe	Ni	Co	Si	Total atoms
standard	M ₂ C	22.5 ±1.7	19.3 ±1.6	14.4 ±1.4	35.7 ±2.0	3.4 ±0.7	4.5 ±0.8	0.2 ±0.2	617 including matrix
	M ₂ C	33.1 ±2.8	28.3 ±2.6	21.2 ±2.2	17.4 ±2.0	-	-	-	Corrected value
overaged	M ₂ C	31.7 ±3.1	37.5 ±3.3	29.9 ±3.1	0.9 ±0.6	-	-	-	220
	MC	40.9 ±4.0	16.9 ±3.0	41.6 ±4.0	0.6 ±0.6	-	-	-	150

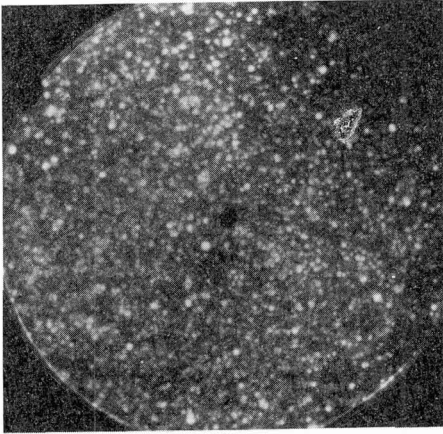


Fig. 1. As-quenched Fe-Ni-C martensite. Neon FIM image 100 K, 12 kV.

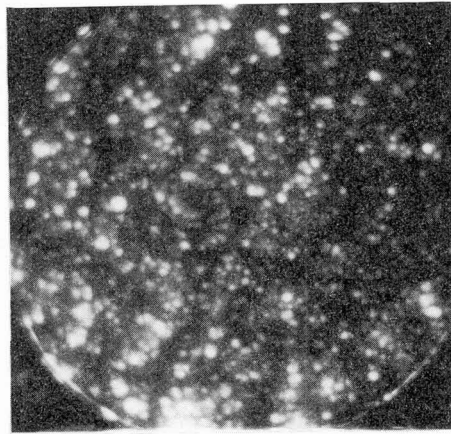


Fig. 2. Fe-Ni-C martensite aged 10 days at room temperature (17 C). Neon FIM image, 100 K, 8.5 kV, showing dark contrast due to periodic carbon-rich regions of composition Fe₃C.

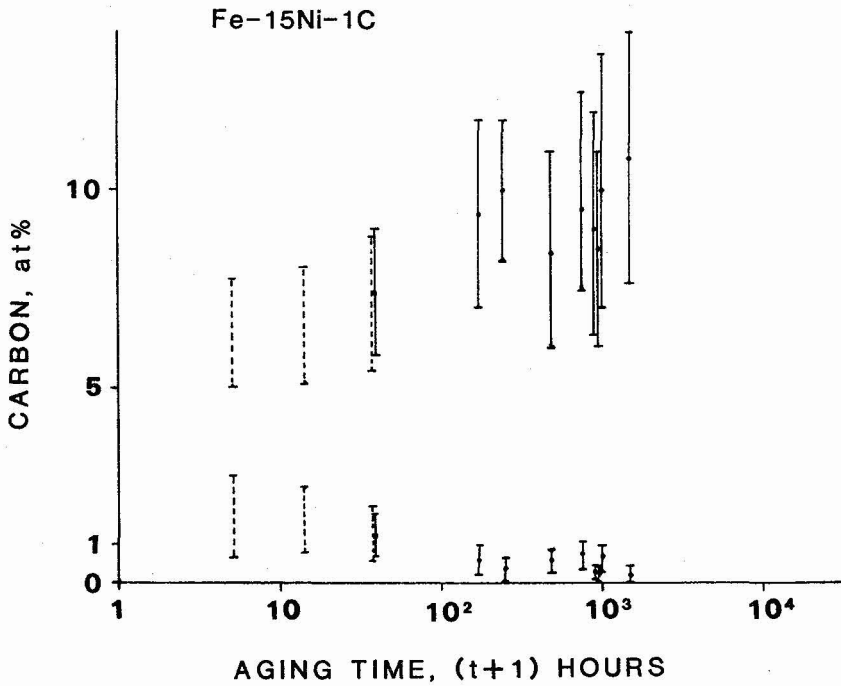


Fig. 3. Increase in amplitude of carbon concentration fluctuations with ageing time at room temperature. Vertical bars indicate the maximum range of peak amplitudes observed.

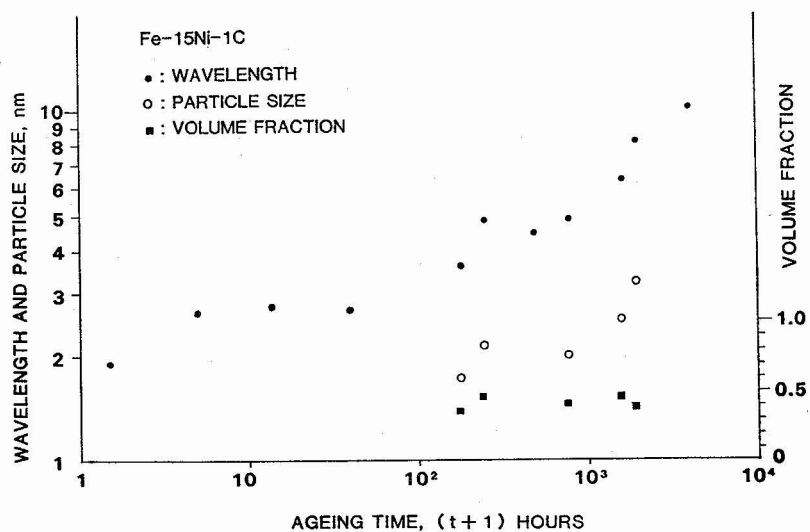


Fig. 4. Increase in wavelength, volume fraction and particle size of carbon rich regions as a function of ageing time at room temperature.

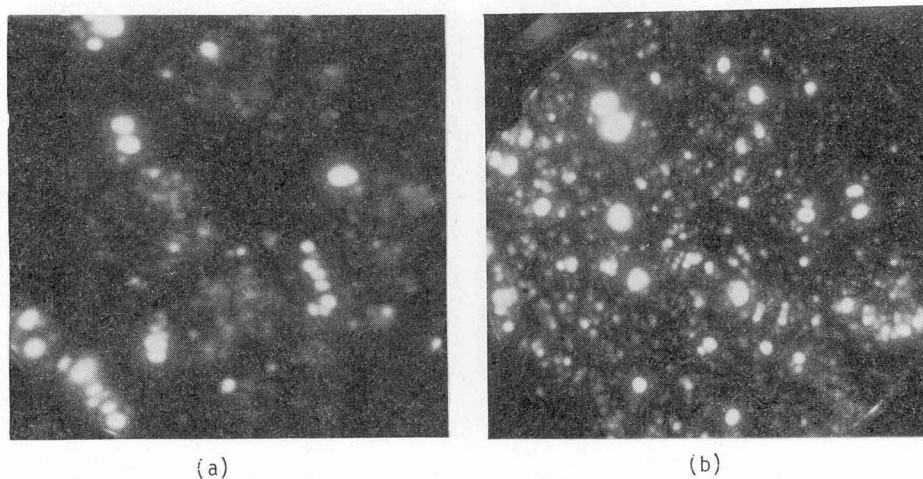


Fig. 5. AF 1410 steel, standard heat treatment condition. Neon FIM image, 100K, showing fine secondary carbide particles (a) below BIV, 5.0 kV, and (b) at BIV, 5.4 kV.

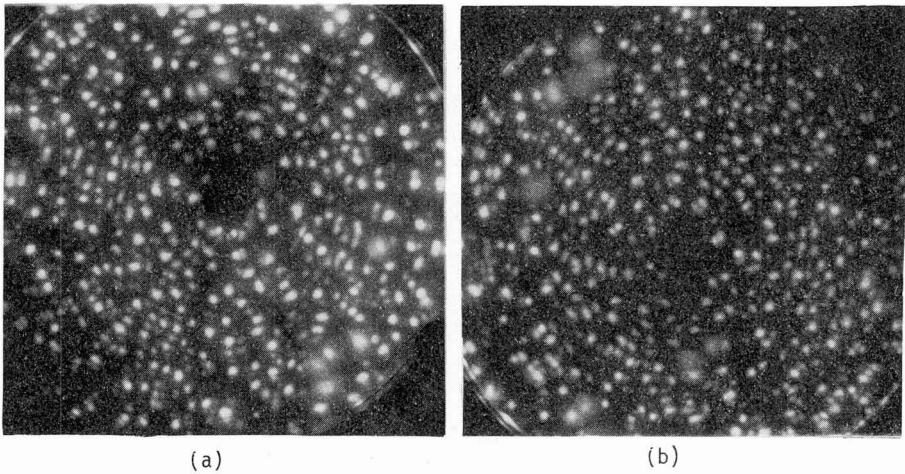


Fig. 6. As Fig. 5, but with images recorded at 50 K and 6.3 kV (BIV). Note ring doubling in central pole of (a), and evidence of a regular superstructure at the extreme left of (b), which may indicate local order in the matrix.

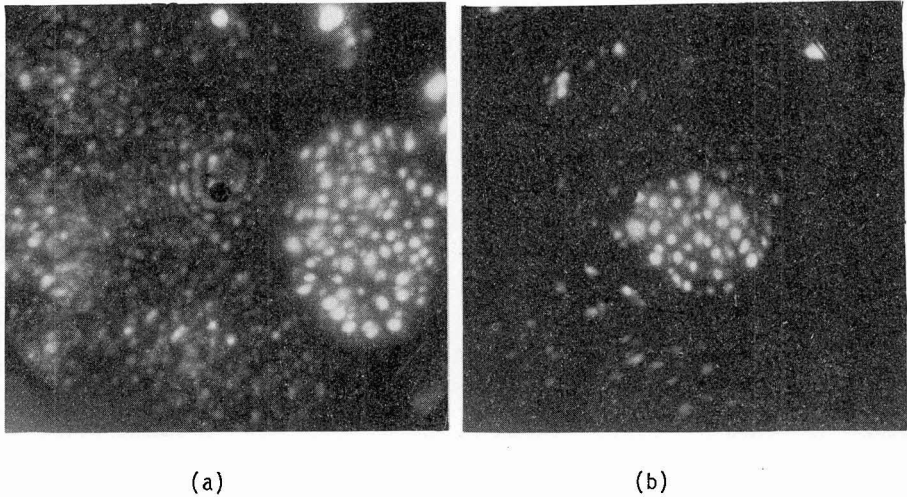


Fig. 7. Overaged AF 1410 steel showing coarse carbides. Neon FIM images, 100 K. (a) M₂C (9 kV), and (b) MC (6 kV).

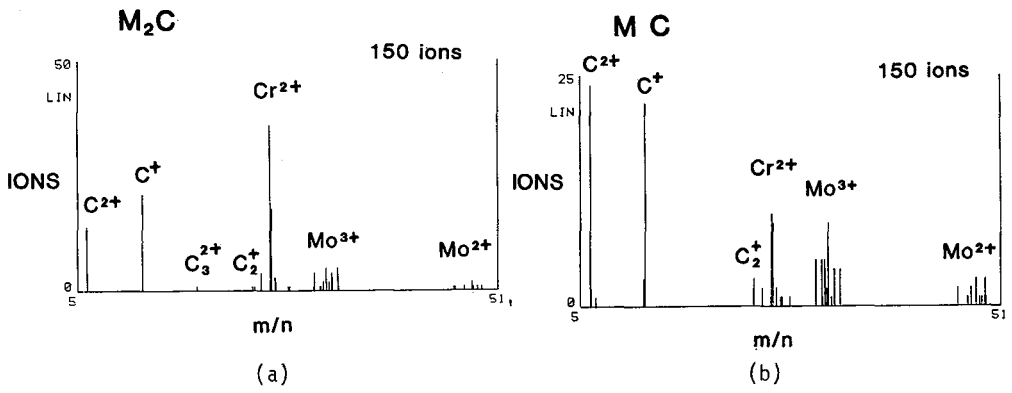


Fig. 8. Atom probe mass spectra from the course carbides shown in Fig. 7., (a) M_2C , and (b) MC .